Observation of a Reflected Shock in an Indirectly Driven Spherical Implosion at the National Ignition Facility

S. Le Pape,[1] L. Divol,[1] L. Berzak Hopkins,[1] A. Mackinnon,[1] N. B. Meezan,[1] D. Casey,[1] J. Frenje,[2] H. Herrmann,[3] J. McNaney,[1] T. Ma,[1] K. Widmann,[1] A. Pak,[1] G. Grimm,[3] J. Knauer,[4] R. Petrasso,[2] A. Zylstra,[2] H. Rinderknecht,[2] M. Rosenberg,[2] M. Gatu-Johnson,[2] and J. D. Kilkenny[5]

[1]*Lawrence Livermore National Laboratory, Livermore, California 94550, USA*

[2]*Plasma Science and Fusion Center, Massachusetts Institute of Technology, Cambridge, Massachusetts 02139, USA*

[3]*Los Alamos National Laboratory, Los Alamos, New Mexico 87545, USA*

[4]*Laboratory for Laser Energetics, University of Rochester, 250 East River Road, Rochester, New York 14623, USA*

[5]*General Atomics Corporation, La Jolla, California 92121, USA*

(Received 8 November 2013; published 4 June 2014)

A 200 μm radius hot spot at more than 2 keV temperature, 1 g/cm^3 density has been achieved on the National Ignition Facility using a near vacuum hohlraum. The implosion exhibits ideal one-dimensional behavior and 99% laser-to-hohlraum coupling. The low opacity of the remaining shell at bang time allows for a measurement of the x-ray emission of the reflected central shock in a deuterium plasma. Comparison with 1D hydrodynamic simulations puts constraints on electron-ion collisions and heat conduction. Results are consistent with classical (Spitzer-Harm) heat flux.

DOI: 10.1103/PhysRevLett.112.225002 PACS numbers: 52.57.Fg, 52.70.La

Central hot spot ignition [1] requires, to reach the appropriate density and temperature, the compression of a millimeter radius cryogenic deuterium-tritium (DT) shell into a 30–40 μm radius hot spot. So far the National Ignition Campaign [2] has been focused on improving the performance of high convergence ratio (> 25) implosions, but the small size of the compressed core as well as the short duration of the implosion have made it challenging to observe the various steps of the hot spot formation. The first step of a central hot spot ignition experiment is the convergence and reflection of a strong spherical shock, ahead of the converging dense shell of thermonuclear fuel and ablator [1].

The shock sequence of a spherical implosion has been theoretically described in papers such as [3–5]. It consists of three phases, first a strong shock travels into the gas, when it gets to the center of the capsule it is reflected on itself, the last phase is the adiabatic compression caused by the shell coming in and compressing the hot spot. In this Letter, we report on the first detailed observation of the second phase of the spherical implosion, when the shock is reflected in a low convergence (5×) indirectly driven implosion under ignition relevant conditions. This was achieved by using a near-vacuum hohlraum to provide a fast rising symmetric drive on a thin (120 μm) plastic capsule reaching very high velocity (> 500 km/s). The ablator acts as a pusher on the high pressure deuterium (DD) or DT fill, launching a strong converging shock that reaches 2 Gbar after rebound. The physics of this system is somewhat similar to that of a direct drive exploding pusher [5], but here we rely on x-ray ablation to transfer energy to a much thicker capsule rather than direct laser isochoric heating of a very thin shell. The results presented in this Letter essentially validate the physics understanding of the following points: (i) An initially near vacuum Au hohlraum can sustain a very efficient x-ray drive [6,7], even when filling with the ablated mass from a capsule. (ii) At low convergence (5×), a correct choice of power balance between various cones of beams allows for the symmetric x-ray drive of a capsule and a nominal 1D implosion. (iii) Once this is achieved, all x-ray and neutron diagnostics are quantitatively reproduced by the radiation-hydrodynamics code HYDRA [8]. (iv) X-ray images of the reflected shock, neutron burn history, and neutron spectrum constrain the heat conduction models in the compressed deuterium plasma and are consistent with a classical Spitzer-Harm (SH) heat flux (nonflux-limited) for this weakly coupled plasma (1 g/cm^3 DD at more than 2 keV temperature). The remainder of this Letter describes the experimental evidence and comparison with numerical modeling.

Experiments of the National Ignition Campaign [7] with gas-filled hohlraums illuminated with 20-ns-long pulses have measured levels of backscattered light due to laser plasma instabilities (LPI) of up to 20%, while vacuum hohlraums with short (2 ns) laser pulses have shown less than 2% backscatter. Typically, though, a high-pressure gas fill (0.96 mg/cm^3 He for standard Rev5 implosions) has been used in hohlraums in order to limit wall expansion, which impedes laser propagation and affects symmetry control [9,10]. For the experiments reported here, 192 frequency-tripled laser beams at a wavelength of 351 nm heat a 30 μm thick gold hohlraum [9.44 mm length, 5.75 mm diameter, 3.1 mm laser entrance holes, Fig. 1(b)] in a 4.3 ns pulse with a peak

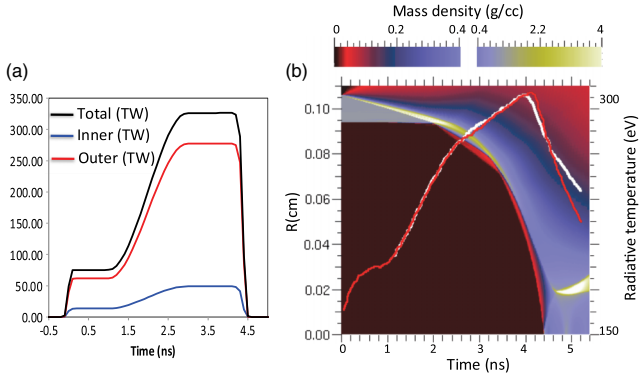

FIG. 1 (color online). (a) Laser pulses: the symmetry of the implosion is achieved with the ratio of inner beam power to total power. For these experiments it is set to 0.15. (b) Measured (white) and simulated (red) x-ray drive and convergence history of the capsule ablator and DD gas. As the shells converge (in yellow), a strong shock (in red) breaks into the DD gas until it is reflected at the center of the capsule.

power of 325 TW and total energy of 933 kJ [Fig. 1(a)]. This laser pulse is short enough that beam propagation is unimpeded throughout the pulse despite extensive hohlraum wall motion and so presents the opportunity to utilize a low gas-fill (low LPI) hohlraum. For cryogenic operation purposes, a nonzero, but very low density (0.032 mg/cm^3) of He fill was utilized. To limit hydrocoupling [11] with the capsule induced by the early-time gold wall expansion and the explosion of the laser entrance hole (LEH) windows, a 2.0 ns 75 TW foot on the laser pulse is introduced; the resulting early x-ray drive ablates enough CH from the capsule to prevent early wall motion from imprinting on the capsule.

The x-ray drive is incident on a spherical capsule with an outer radius of 1055 μm $\pm$ 5 μm, and with a 120 μm $\pm$ 1 μm thick ablator, consisting of multilayered plastic (CH) with a graded silicon dopant, filled either with pure DD gas at a density of 6.33 mg/cm^3 or DT gas at 7.66 mg/cm^3, maintaining equal number density between the two fuel gases. The capsule absorbs x rays from the hohlraum for several ns before burning through, when the radiation front completely penetrates the ablator. At this point, the ablator peak velocity reaches 550 km/s and a single strong shock is launched into the gas fuel that stagnates at the center [Fig. 1(c)], generating nuclear yield after reflexion. Total measured backscatter was less than 1%, for a laser to hohlraum coupling of 99%. The x-ray drive delivered by this pulse gave a peak radiation temperature measured by DANTE [12] of 293 eV $\pm$ 5 eV. As shown in Fig. 1(c), the experimental x-ray drive as a function of time (white curve) is accurately described by the HYDRA NLTE detailed configuration accounting (DCA) high flux model without multipliers (red curve) [7,13]. Notably, the x-ray drive is sustained until bang time, i.e., peak compression (4.82 ns), even as the hohlraum fills with the CH ablator plasma.

The performance of these implosions was diagnosed using a suite of x-ray and nuclear diagnostics [14]; a summary of the DT and DD performance compared to integrated HYDRA calculations is shown in Table I. Following good agreement between measured and calculated x-ray drive, the measured bang time is within 80 ps of the calculated one, with correct convergence ratios and ion temperatures. As a result, both for the DD and DT implosion, the experimentally measured yield normalized to the 1D simulated yield (yield over clean) is essentially 1, demonstrating 1D performance. Because the convergence of the implosion is low, the areal density ρR achieved at bang time can be accurately characterized using secondary nuclear reactions. A total $\rho R = 44 \pm 7$ mg/cm^2, similar to the 45 to 60 mg/cm^2 range from the HYDRA simulations has been measured. In addition, the fuel ρR can also be inferred from the ratio of the secondary DT neutron production to the primary DD neutron yield, as measured by the neutron time-of-flight detectors [15]. As the ablator is almost completely ablated, the shell is transparent to the emission of the hot spot near bang time.

In high convergence, high ρR experiments on the National Ignition Facility, the symmetry of the compressed core is tuned through the cross beam energy transfer process between inner and outer beams induced by a wavelength separation between cones of laser beams [16]. Because of the hot, low density plasma inside the vacuum hohlraum,

TABLE I. Summary of the performance of the DD implosion (N131203) and the DT implosion (N130503) compared to the corresponding integrated HYDRA simulations.

	N130312	N130503	HYDRA postshot
DD neutron yield	$5.1 \times 10^{12} \pm 1.6 \times 10^{11}$		4.3×10^{12}
DT neutron yield		$5.12 \times 10^{14} \pm 9 \times 10^{12}$	5×10^{14}
DD T_{ion} (keV)	3.5 ± 0.2		3.53
DT T_{ion} (keV)		4.6 ± 0.2	4.6
X-ray bang time (ns)	4.82 ± 0.1	Identical	4.74
M_0 Fourier mode (μm)	197 ± 6	Identical	200
Peak radiation temperature (eV)	293 ± 5	Identical	290
Fuel ρR	16 ± 2 mg/cm^2	Identical	15.5 ± 1.6 mg/cm^2
Fuel+ablator ρR	52 ± 8 mg/cm^2	Identical	44 ± 7 mg/cm^2

cross beam energy transfer is predicted to be negligible when the wavelength difference between the inner and outer cones is set to zero. The symmetry of the implosion is thus directly controlled using the power balance between the inner and outer beams [see Fig. 1(a)]. The time integrated x-ray images above 4 keV [Fig. 2] show a very round implosion with Fourier modes $M = 2$–4 below 0.5% and a hot spot radius $M_0 = 200$ μm (as compared to approximately 25 μm for comparable high convergence implosions on National Ignition Facility). The corresponding unscattered neutron image [measured by the neutron imaging system (NIS) [17] on the DT shot], is notably smaller at a radius close to 90 μm. This is predicted by HYDRA simulations and can be explained by two phenomena: first the reflected shock cools as it expands radially, then the outer part of the hot spot is cooled by heat conduction into the surrounding ablator plasma during the confinement period. The neutron production rate (as measured by the NIS) drops sharply at a radius where the ion temperature does not reach above 2.5 keV during the implosion (a temperature at which the D-T cross section sharply drops).

The dynamics of the DD implosion are well captured by a gated x-ray detector (GXD) along the north polar axis measuring the capsule x-ray emission above 4 keV. The time resolved x-ray brightness is absolutely cross calibrated using time integrated image plate images [18] allowing a direct comparison with simulations. In addition, on the DT implosion the neutron burn history is measured using the γ-ray history detector (GRH) [19]. Both x-ray emission history and neutron burn history are plotted in Fig. 3. The neutron burn history exhibits a very sharp rise at shock flash, when maximum ion temperature is reached. Peak burn rate is reached just before the reflected shock hits the ablator, at a time when the entire volume of fuel has been heated, almost maximum compression is obtained, and before heat conduction losses and decompression happen.

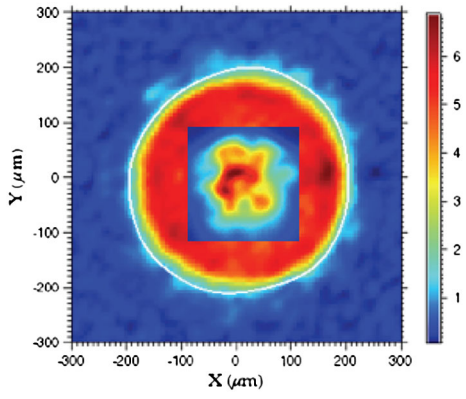

FIG. 2 (color online). Time integrated x-ray (above 4 keV) and unscattered neutron images of the DT implosion. The neutron image (inset) size is half the size of the x-ray image due to the temperature gradient int the hot spot.

It is followed by a long (400 ps) tail corresponding to a progressive drop in ion temperature. The x-ray emission shows a relatively slower start, increasing with the volume of DD plasma heated by the rebound shock, reaching a maximum when the inner shell of dense CH ablator is heated above 1 keV and Bremsstrahlung emission from electron–carbon-ion collisions dominates. HYDRA simulations closely match both neutron and x-ray emission histories, validating the simulated ion temperature (GRH) and electron temperature (GXD). The simulation underestimates the peak x-ray emission coming from the CH ablator by ~50%, which could indicate uncertainties in the modeling of the sharp interface between DD and CH, or in the propagation of the reflected shock through the initially dense (> 4 g/cm^3) and cold ($T_e = T_i \approx 300$ eV) stagnating ablator shell.

Figure 4 summarizes the different phases of the implosion, as simulated and measured by the polar gated x-ray imager (described above, with a magnification of 4× through 30 μm pinholes) for the DD implosion. The good quantitative agreement with simulations allows a more detailed study of the reflected shock as it propagates outward through the deuterium fuel. Taking advantage of the rotational symmetry evident in Fig. 4, one can obtain instantaneous radial profiles of the x-ray emission and directly observe the propagation of the reflected shock. Figure 5 shows the dynamics through three snapshots separated by 40 ps each. The finite bandwidth of the simulated data corresponds to the error bar of the simulation considering an experimental jitter of the x-ray gated imager of 10 ps. This evolution is well reproduced by HYDRA simulations using SH heat conduction [20] with no flux limiter. By comparison, artificially reducing heat conduction leads to a faster, steeper shock while increasing it leads to a slower shock with a longer precursor. During the propagation of the shock, the deuterium plasma has an ion temperature evolving from 3–8 keV, an electron temperature $T_e = [2$–$4]$ keV and density $\rho = [0.5$–$1]$ g/cm^3. The total pressure is around 2 Gbar.

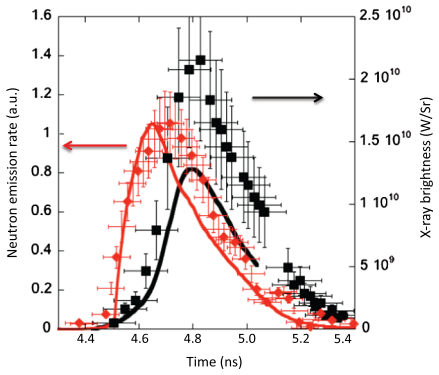

FIG. 3 (color online). Measured (symbols) and calculated (lines) x-ray (black) and neutron (red) emission from the low convergence implosion.

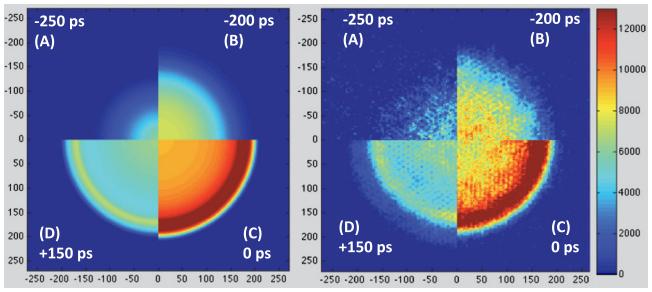

FIG. 4 (color online). Simulated (left) and measured (right) x-ray images of the DD implosion. Simulations absolute values have been multiplied by 1.3 and plotted on the same absolute scale. The converging shock reaches the origin (A), bounces back and expands outward [(B) time of peak neutron emission]. Peak x-ray emission happens once the shock heats the in-falling CH ablator (C). Shock reflection on the ablator and continuing compression reheat the center while the outgoing shock lights up the Si dopant in the outer layers of the ablator (D). The color bar is in arbitrary units. The (A) and (B) images are multiplied by a 2.5 factor to increase their visibility.

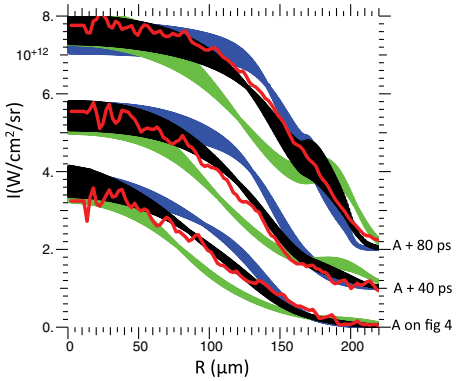

FIG. 5 (color online). Rebound shock x-ray emission (above 4 keV) radial profile measurements (red curves, slim curve, from polar GXD) at three times separated by 40 ps (vertically offset for visibility) before reaching the CH shell. Comparison to simulations using SH electron and ion heat conduction (black), 2× (respectively, 0.5×) electron-ion collision rate in green, lower (respectively, blue, upper). Simulations are normalized to match the middle curve.

For time-averaged values ($T_i = 4$ keV, $T_e = 3$ keV, $\rho = 1$ g/cm^3), a deuterium plasma is in a weakly coupled regime ($N_D = 500$), with the Coulomb logarithms $\lambda_{ee} = \lambda_{ei} = 5$ and $\lambda_{ii} = 8.4$. Hence classical binary Coulomb collisions should dominate the transport processes. Typical collisional times are $\tau_e = 0.04$ ps and $\tau_i = 3$ ps, so one expects near-Maxwellian distribution functions for both deuterons and electrons at the hydrodynamics time scale of 10 ps (the shock propagates outward for 100 ps). On the other hand, the electron-ion equilibration time is of the order of 100 ps, leading to a nonequilibrium system: T_i relates to the shock strength, T_e to the compression and for longer times to the equilibration rate with ions. The effective electron and ion mean free paths are of the order of 0.1 μm, much shorter than the temperature gradient scale length (30 μm) once the shock has propagated a similar distance, which is in the valid domain of the SH perturbation theory [20]. Of course, this condition is violated at exact convergence in one-dimensional simulations, but only for a very short time (< 30 ps) and a very small volume (radius < 30 μm), and thus does not affect measurable observables. Three-dimensional simulations would further limit point convergence.

While x-ray emission is related to T_e, simulated profiles are also sensitive to ion temperature through the electron-ion temperature equilibration. Furthermore, neutron yield and temperature are directly related to T_i, and can be used to independently constrain heat conduction modeling. While SH heat conduction leads to good agreement with the experiment (see Table I), reducing by a factor of 2 the SH conductivity leads to an increase of the neutron yield by $2.5 10^{14}$ and T_i by 600 eV, both outside of the measurement error bars (see Fig. 3), decreasing the SH conductivity by a factor 2 has the opposite effect. The combination of these two independent measurements constrains the heat conduction model for the hot spot around shock flash to ±50% of the theoretical value. This validation extends to higher convergence (> 20×), higher density (30–100 g/cm^3) ignition relevant implosion, where all validity conditions stated above will still be fulfilled.

In summary, we have observed for the first time the reflection phase of a spherical implosion in a 2 keV, 1 g/cm^3 plasma, providing insight on the thermal conductivity in an ignition relevant hot, dense DD plasma. The precise capture of the dynamics of the reflected shock x-ray emission, coupled to neutron diagnostics, are consistent with (nonflux limited) Spitzer-Harm theory within the framework of 1D hydrodynamics. This provides a theoretical and numerical framework to design a higher-convergence cryogenic layered DT implosion driven by a vacuum hohlraum. This high efficiency, LPI-free hohlraum platform could drive a high density carbon capsule to velocity approaching 400 km/s, at convergence more than 20×. For a cryogenic layered DT implosion, this would result in a hot spot pressure of 200 Gbar and noticeable α heating.

This work was performed under the auspices of the U.S. Department of Energy by Lawrence Livermore National Laboratory under Contract No. DE-AC52-07NA27344. Work was also supported by the Laboratory Directed Research and Development Grant No. 11-ERD-050 and the National Laboratory User Facility.

[1] J. D. Lindl, P. Amendt, R. L. Berger, S. G. Glendinning, S. H. Glenzer, S. W. Haan, R. L. Kauffman, O. L. Landen, and L. J. Suter, Phys. Plasmas **11**, 339 (2004).

[2] O. L. Landen, J. Edwards, S. W. Haan, H. F. Robey, J. Milovich, B. K. Spears, S. V. Weber, D. S. Clark, J. D. Lindl, B. J. MacGowan *et al.*, Phys. Plasmas **18**, 051002 (2011).
[3] L. D. Landau and E. M. Lifshitz, *Fluids Mechanics* (Addison-Wesley, Reading, MA, 1959).
[4] V. G. Guderley, Luftfahrtforschung **19**, 302 (1942).
[5] B. Ahlborn, Phys. Fluids **25**, 541 (1982).
[6] S. Glenzer, B. MacGowan, N. Meezan, P. Adams, J. Alfonso, E. Alger, Z. Alherz, L. Alvarez, S. Alvarez, P. Amick *et al.*, Phys. Rev. Lett. **106**, 085004 (2011).
[7] J. L. Kline, S. H. Glenzer, R. E. Olson, L. J. Suter, K. Widmann, D. A. Callahan, S. N. Dixit, C. A. Thomas, D. E. Hinkel, E. A. Williams *et al.*, Phys. Rev. Lett. **106**, 085003 (2011).
[8] M. M. Marinak, G. D. Kerbel, N. A. Gentile, O. Jones, D. Munro, S. Pollaine, T. R. Dittrich, and S. W. Haan, Phys. Plasmas **8**, 2275 (2001).
[9] N. D. Delamater, T. J. Murphy, A. A. Hauer, and R. L. Kauffman, Phys. Plasmas **3**, 2022 (1996).
[10] R. L. Kauffman, L. V. Powers, S. N. Dixit, and S. G. Glendinning, Phys. Plasmas **5**, 1927 (1998).
[11] D. E. Hinkel, S. W. Haan, A. B. Langdon, T. R. Dittrich, C. H. Still, and M. M. Marinak, Phys. Plasmas **11**, 1128 (2004).
[12] E. L. Dewald, K. M. Campbell, R. E. Turner, J. P. Holder, O. L. Landen, S. H. Glenzer, R. L. Kauffman, L. J. Suter, M. Landon, and M. Rhodes, Rev. Sci. Instrum. **75**, 3759 (2004).
[13] R. E. Olson, L. J. Suter, J. L. Kline, D. A. Callahan, M. D. Rosen, S. N. Dixit, O. L. Landen, N. B. Meezan, J. D. Moody, C. A. Thomas *et al.*, Phys. Plasmas **19**, 053301 (2012).
[14] M. J. Edwards, J. D. Lindl, B. K. Spears, S. V. Weber, L. J. Atherton, D. L. Bleuel, D. K. Bradley, D. A. Callahan, C. J. Cerjan, D. Clark *et al.*, Phys. Plasmas **18**, 051003 (2011).
[15] V. Y. Glebov, D. D. Meyerhofer, T. C. Sangster, C. Stoeckl, S. Roberts, C. A. Barrera *et al.*, Rev. Sci. Instrum. **77**, 10E715 (2006).
[16] P. Michel, L. Divol, E. A. Williams, C. A. Thomas, D. A. Callahan, S. Weber, S. W. Haan, J. D. Salmonson, N. B. Meezan, O. L. Landen *et al.*, Phys. Plasmas **16**, 042702 (2009).
[17] F. E. Merrill, D. Bower, R. Buckles, D. D. Clark, C. R. Danly, O. B. Drury, J. M. Dzenitis, V. E. Fatherley, D. N. Fittinghoff, R. Gallegos *et al.*, Rev. Sci. Instrum. **83**, 10D317 (2012).
[18] T. Ma, N. Izumi, R. Tommasini, D. K. Bradley, P. Bell, C. J. Cerjan, S. Dixit, T. Doppner, O. Jones, and J. L. Kline, Rev. Sci. Instrum. **83**, 10E115 (2012).
[19] H. W. Herrmann, N. Hoffman, D. C. Wilson, W. Stoeffl, L. Dauffy, Y. H. Kim, A. McEvoy, C. S. Young, J. M. Mack, C. J. Horsfield *et al.*, Rev. Sci. Instrum. **81**, 10D333 (2010).
[20] J. F. Luciani, P. Mora, and J. Virmont, Phys. Rev. Lett. **51**, 1664 (1983).